Photoacoustics 31 (2023) 100515

Contents lists available at ScienceDirect

Photoacoustics

journal homepage: www.elsevier.com/locate/pacs

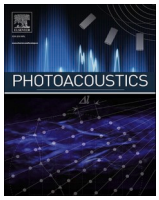

Highly sensitive light-induced thermoelastic spectroscopy oxygen sensor with co-coupling photoelectric and thermoelastic effect of quartz tuning fork

Cunguang Lou [a], Jialiang Dai [a], Yaxin Wang [a], Yu Zhang [a], Yifan Li [a], Xiuling Liu [a,*], Yufei Ma [b,*]

[a] College of Electronic Information and Engineering & Hebei Key Laboratory of Digital Medical Engineering, Hebei University, Baoding 071000, China
[b] National Key Laboratory of Science and Technology on Tunable Laser, Harbin Institute of Technology, Harbin 150001, China

ARTICLE INFO

Keywords:
Light-induced thermoelastic spectroscopy
Quartz tuning fork
$CH_3NH_3PbI_3$ perovskite
Oxygen
Gas detection

ABSTRACT

A light-induced thermoelastic spectroscopy (LITES) gas detection method based on $CH_3NH_3PbI_3$ perovskite-coated quartz tuning fork (QTF) was proposed. By coating $CH_3NH_3PbI_3$ thin film on the surface of ordinary QTF, a Schottky junction with silver electrodes was formed. The co-coupling of photoelectric effect and thermoelastic effect of $CH_3NH_3PbI_3$-QTF results in a significant improvement in detection performance. The oxygen (O_2) was select as the target analyte for measurement, and experimental results show that compared with the commercial standard QTF, the introduction of $CH_3NH_3PbI_3$ perovskite Schottky junction increases the 2*f* signal amplitude and signal-to-noise ratio (SNR) by ~106 times and ~114 times, respectively. The minimum detection limit (MDL) of this LITES system is 260 ppm, and the corresponding normalized noise equivalent absorption coefficient (NNEA) is 9.21×10^{-13} $cm^{-1}\cdot W\cdot Hz^{-1/2}$. The Allan analysis of variance results indicate that when the average time is 564 s, the detection sensitivity can reach 83 ppm. This is the first time that QTF resonance detection has been combined with perovskite Schottky junctions for highly sensitive optical gas detection.

1. Introduction

Oxygen (O_2) is one of the main components of air. Human cannot live without oxygen, and it also has a very important significance for industrial production, food packaging, biomedical technology, and environmental monitoring [1–3]. Therefore, it is of great importance to carry out O_2 concentration detection with fast response and high sensitivity. Currently, one of the most widely used O_2 detection methods are electrochemical sensors [4,5]. Unfortunately, disadvantages of electrochemical O_2 sensors, such as aging and contamination have limited their application in many fields.

Laser absorption spectroscopy is based on the absorption properties of target molecules. Due to its unique advantages such as high selectivity, stability, and real-time online continuous monitoring [6–9], it has been widely used in the field of gas detection. Sensors based on laser absorption spectroscopy, such as tunable diode laser absorption spectroscopy (TDLAS), photoacoustic spectroscopy (PAS), and quartz enhanced photoacoustic spectroscopy (QEPAS) have been applied for the detection of various gases [10–18]. Among them, QEPAS was first proposed in 2002, using a quartz tuning fork (QTF) instead of a microphone as an acoustic detection element to improve the sensitivity [19]. However, QEPAS is a contact measurement technology and the QTF needs to be placed in gas cell, making it difficult to achieve photoelectric separation, which limits its application in corrosive gas detection. Light-induced thermoelastic spectroscopy (LITES) was first proposed in 2018 [20], the method does not require direct contact of the QTF with the detection gas. In addition, the commercial standard QTF is small, cheap, and has ultra large wavelength response range, so LITES is widely used in gas detection in recent years [21–30].

The characteristics of the QTF directly affect the performance of the LITES system, various strategies have been proposed to improve the LITES's sensitivity. A custom QTF with a lower resonant frequency and larger fork-spaced T-shape arms were shown to be able to reduce background noise and improve sensor performance [31,32]. Qiao et al. used a custom T-shaped QTF for the LITES sensor and achieved a 5-fold improvement in CO detection sensitivity over TDLAS system [33]. The thermoelastic signal's amplitude is proportional to the light absorption of the QTF, and the deposition of highly absorbing material on the QTF surface can improve the sensitivity [34,35]. In addition, to improve the photothermal conversion efficiency, polymeric materials with high

* Corresponding authors.
E-mail addresses: liuxiuling121@hotmail.com (X. Liu), mayufei@hit.edu.cn (Y. Ma).

https://doi.org/10.1016/j.pacs.2023.100515
Received 14 April 2023; Received in revised form 11 May 2023; Accepted 22 May 2023
Available online 23 May 2023

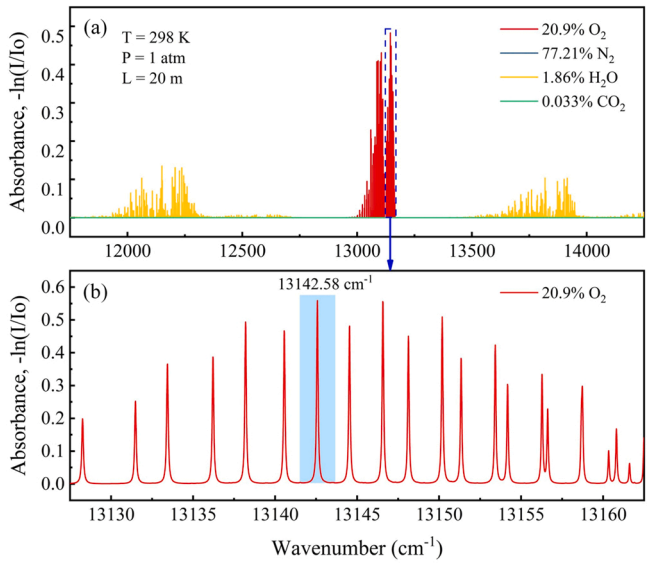

Fig. 1. (a) Simulated absorption lines of the main atmospheric components according to the HITRAN database. (b) the strongest O_2 absorption line is located at about 13,142 cm^{-1}.

thermal expansion coefficient were coated on QTF prongs [36,37]. But the surface coating method has its own shortcomings, such as too thick coating will reduce the quality factor (Q) and the detection sensitivity of the QTF sensor. In general, these strategies improve the sensitivity within 10 times magnification.

In this work, we reported a LITES sensor using a $CH_3NH_3PbI_3$-coated QTF. To overcome the above shortcomings of QTF sensors, a perovskite material with both photoelectric and photothermal effects was used for the surface coating of commercial standard QTF. By coupling the photoelectric effect and thermoelastic effect onto the QTF, combined with a 20 m path length gas cell and wavelength modulation spectroscopy technology, the sensitivity of the LITES system was improved effectively. The performance of surface coated QTF sensors was validated using O_2 as the target gas, the 2*f* signal amplitude and signal-to-noise ratio (SNR) of $CH_3NH_3PbI_3$-QTF were experimentally studied and compared with standard commercial QTF.

2. Experimental setup

2.1. Absorption line selection

Due to the presence of the fingerprint spectrum of gas molecules, the LITES technology based on Beer Lambert's law enables excellent selectivity as well as real-time measurement. The selected gas absorption spectral line should have a strong absorption intensity, and there should be no interference from other gases near the selected absorption spectral line. According to simulation of the HITRAN database and SpectraPlot website, the relatively strong absorption spectral line of O_2 is located around 13,000 cm^{-1} [38], as shown in Fig. 1. Fig. 1(a) shows the absorption spectra of the main components and contents of the atmosphere at 298 K, 1 atm, and for an absorption pathlenght of 20 m. As can be seen from the figure, the absorption spectral line at 13,142.58 cm^{-1} (760.88 nm) meets the line selection principle, and the absorption line strength for this peak is 8.74×10^{-24} $cm^{-1}/(mol \cdot cm^{-2})$ [39], and there will be no interference from other gases here. Therefore, the absorption spectral line here was selected for the experiment.

2.2. LITES sensor system experimental device

A schematic diagram of the $CH_3NH_3PbI_3$-QTF LITES sensor for gas detection is shown in Fig. 2. A 760 nm vertical-cavity surface-emitting laser (VCSEL, EP760-VC-TP39) with a maximum laser power of 1 mW was selected as the wavelength scanning laser source. The wavelength of the VCSEL laser was modulated by adjusting the injection current and the operating temperature. In the experiment, the driving current was controlled by the customized LDTC0520 driver, and the laser temperature was set to 25 °C. The drive signal was the superposition of a sine wave and a sawtooth signal generated by a dual channel function generator (Tektronix, AFG3022C). First, the laser beam was collimated and then enters a Herriott gas cell with a length of about 20 m. A commercially available quartz crystal oscillator with a nominal resonant frequency (f_0) of 32,768 Hz was selected for shelling to obtain a traditional QTF detector. The laser beam output from the gas cell was focused on the root of the QTF to excite a larger thermoelastic signal. The current of the QTF was firstly amplified by a 3 MHz bandwidth trans-impedance amplifier (AD712JR), the harmonic signal was then demodulated by a lock-in amplifier (Stanford Research Systems, SR830) and collected by an oscilloscope (Tektronix, MDO3012). Throughout the experiment, the lock-in amplifier sensitivity was set at 50 mV to ensure the consistent signal gain. The filter slope was set to 12 dB/oct and the time constant was set to 10 ms.

In this paper, wavelength modulated spectroscopy and second harmonic (2*f*) were utilized to achieve highly sensitive detection of O_2. In the experiment, high-frequency (~16 kHz) sine waves are superimposed on low-frequency (0.5 Hz) sawtooth wave scanning signals. The low-frequency sawtooth wave allows the laser wavenumber to pass through the selected O_2 absorption line. The high-frequency sine wave is used to modulate the laser density, transferring the low-frequency concentration dependent absorption signal to the high-frequency, which can effectively suppress noise in the low-frequency region.

2.3. Design of the photoelectric and thermoelastic co-coupling QTF sensor

The $CH_3NH_3PbI_3$ perovskite light absorbing layer was prepared

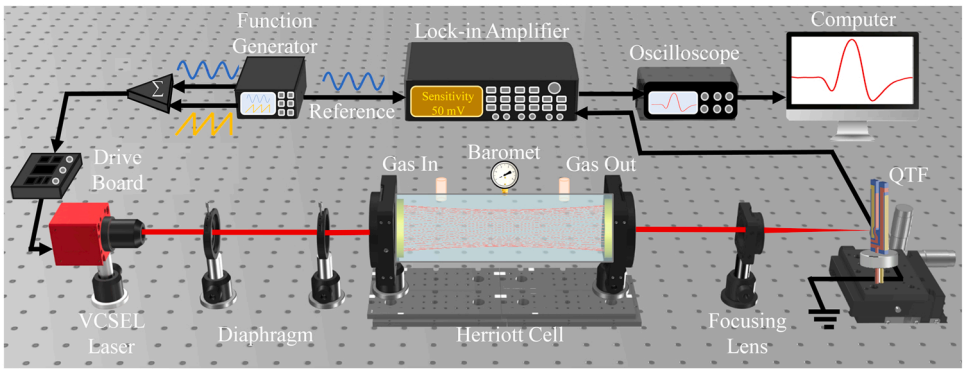

Fig. 2. Schematic diagram of the LITES gas detection system.

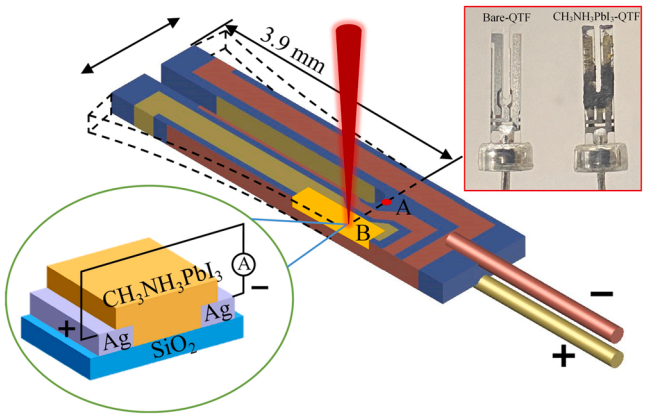

Fig. 3. Structural diagram of the photoelectric-thermoelastic co-coupling QTF sensor.

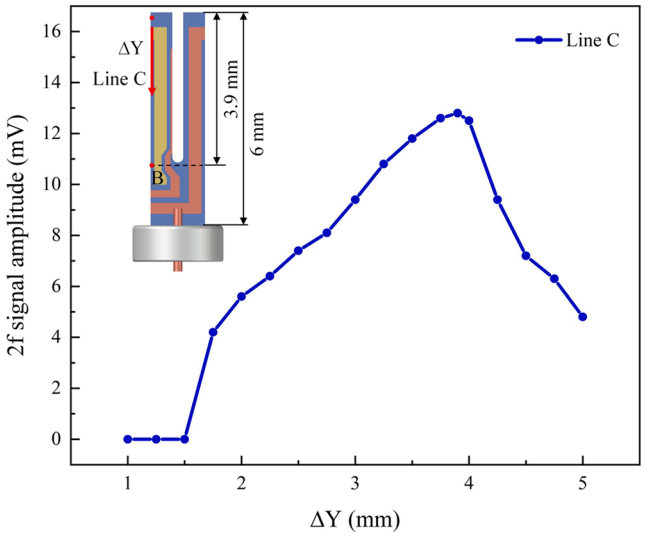

Fig. 4. The 2 *f* signal amplitude at different excitation positions of QTF.

between two different electrodes on the QTF surface by a one-step spin coating method. By dropping $CH_3NH_3PbI_3$ solution onto the surface of QTF and using a spin coating machine for spin coating, a perovskite thin film is obtained. In terms of details, firstly, we prepared the methylammonium iodide (CH_3NH_3I) and leaded iodide (PbI_2) dissolved solution with molar ratio of 1:1. Secondly, we prepared the N, N-dimethylformamide (DMF) and dimethyl sulfoxide (DMSO) mixed solvent with a volume ratio of 4:1, after mixing the solution with the solvent, and stirred at room temperature for 5 h, obtaining the yellow transparent $CH_3NH_3PbI_3$ perovskite precursor solution. Thirdly, we welded the QTF to a custom meta-disk and attached them to the spin coater (EZ4-S-PP, Lebo); we dropped the $CH_3NH_3PbI_3$ perovskite precursor solution onto the surface of the QTF, and spined coated at 1000 rpm for 10 s. Finally, the QTF was placed in a vacuum drying oven and heated at 100 °C for 30 min to complete the fabrication of $CH_3NH_3PbI_3$ perovskite thin films on it.

A commercial QTF with a resonance frequency of 32.76 kHz was chosen as the detector. Fig. 3 shows the structural diagram of the photoelectric and thermoelastic co-coupling QTF, and the illustration shows the bare QTF and the QTF coated with $CH_3NH_3PbI_3$ film. The QTF has two vibration prongs that consist of the silica substrate and the silver surface, and two pins connect the silver on upper and lower surfaces, respectively. Normally, the maximum excitation position of the thermoelastic effect is located at point A [40]. However, there are no

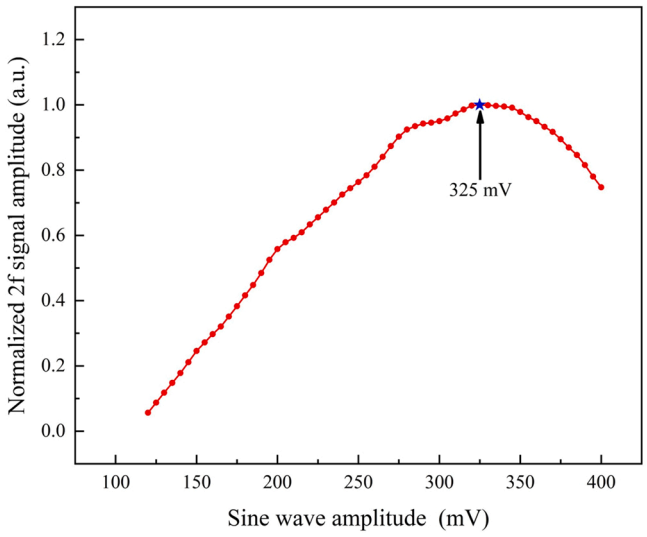

Fig. 5. Functional relationship between 2*f* signal amplitude and sine wave amplitude.

adjacent two different electrodes around point A to form an Ag/$CH_3NH_3PbI_3$/Ag Schottky structure, resulting in the absence of two different electrodes to collect the photocurrent generated by the photoelectric effect. As shown in the inset figure of Fig. 3, the surface area of the side edge of QTF is silica, with different electrodes on both sides. After coating with perovskite film, this can form a Schottky structure, as shown in point B in the figure. It is well known that photoelectric effect generation is attributed to the electron-hole pairs excited by the incident photon energy which is larger than the band gap of materials. There is a depletion region at the interfaces of the Ag and $CH_3NH_3PbI_3$ due to differences in energy level of the two materials. The energy gap of $CH_3NH_3PbI_3$ determined from the valence band and conduction band is about 1.5 eV, which ensure the light with wavelength less than 826 nm is sufficient to excite electron-hole pairs and subsequent charger carrier transport. The laser light source we used has a central wavelength of about 760 nm, so when this laser irradiates the surface of the QTF coated with $CH_3NH_3PbI_3$ perovskite, it can produce the photoelectric effect very well.

Experiment was conducted to investigate the most sensitivity region of the QTF, and the results are shown in Fig. 4. The zero point of Y axis is located at the top of the QTF, and the measurement was conducted on different positions along line C. It can be seen that the least sensitive position located at the tip of the QTF, while the most sensitive position located at the bottom of the QTF. When $\Delta Y = 3.9$ mm, the thermoelastic signal reaches the maximum value, which is consistent with the results of studies in the literature [20,25,26]. Therefore, point B was selected as the optimal photoexcitation position. The thermoelastic effect here is only inferior to point A. There are different pins on both sides, and this point also provides a Schottky structure for photoelectric detection. Therefore, this point B was selected as the optimal location for perovskite coating.

3. Experimental results and discussion

The wavelength modulation depth is an important parameter in wavelength modulation spectroscopy based sensing system. To realize optimal detection sensitivity, the laser wavelength modulation depth was optimized at first. The modulation depth is related to the amplitude of the high-frequency sine wave. By adjusting the sine wave amplitude, the optimal 2*f* signal can be obtained. Experiment was conducted to measure the functional relationship between the amplitude of the 2*f* signal and the high-frequency sine wave. As shown in Fig. 5, the 2*f* signal amplitude first increases and then decreases as the sine wave amplitude

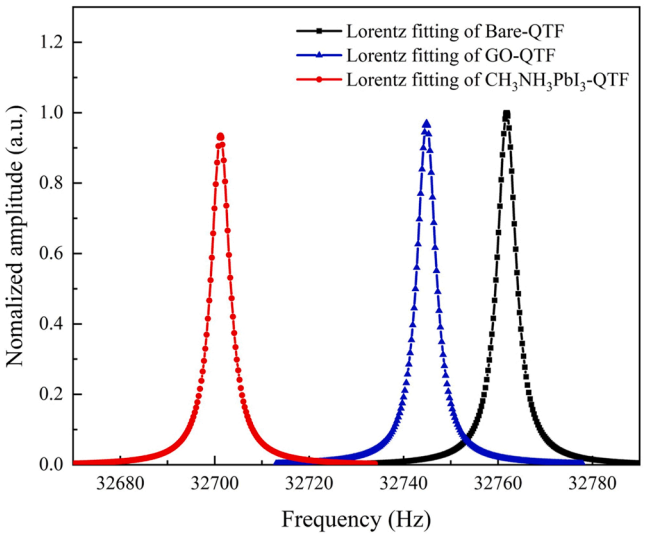

Fig. 6. Frequency response for the Bare-QTF (black line), GO-QTF (blue line) and $CH_3NH_3PbI_3$-QTF (red line), respectively.

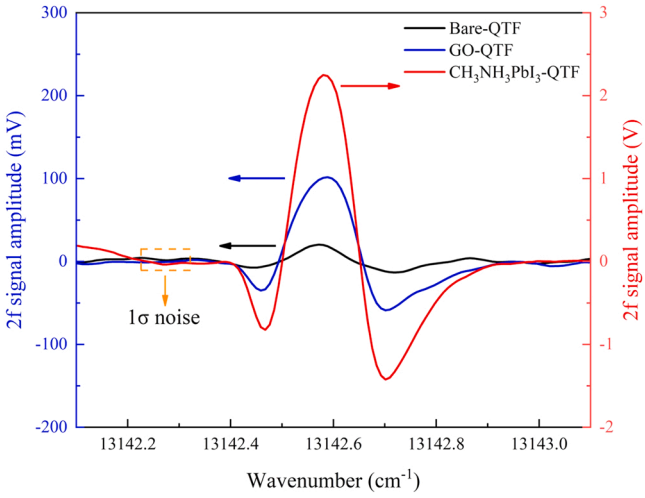

Fig. 7. 2*f* signal of three different types of QTFs.

increases. When the sine wave amplitude was 325 mV, the 2*f* signal reached the maximum. This modulation depth was used in the subsequent experiments to obtain optimal system performance.

Graphite oxide (GO) has a strong absorption coefficient, and coating GO on QTF (GO-QTF) can improve the absorption of laser, thus improving the thermoelastic effect [35]. However, $CH_3NH_3PbI_3$ perovskite not only has a strong absorption coefficient, but also coating $CH_3NH_3PbI_3$ on QTF ($CH_3NH_3PbI_3$-QTF) can generate photoelectric effects, thus greatly improving the detection sensitivity. To compare the sensitivity of GO-QTF with only thermoelastic effects and $CH_3NH_3PbI_3$-QTF with co-coupled thermoelastic and photoelectric effects, GO and $CH_3NH_3PbI_3$ were coated on bare QTF (Bare-QTF) respectively. The film coating may affect the QTF's vibration state, by scanning the frequency of the sinusoidal modulation signal around 32.7 kHz, the resonant frequency in the testing environment was retrieved. The characteristics of three kinds QTFs were measured to obtain resonance frequencies and related Q value. The frequency responses of these three kinds of QTFs were normalized and fitted with the Lorentz function, and the results are shown in Fig. 6. As can be seen, the resonance frequencies of Bare-QTF, GO-QTF and $CH_3NH_3PbI_3$-QTF are 32,762 Hz, 32,745 Hz and 32,701 Hz, respectively, with corresponding

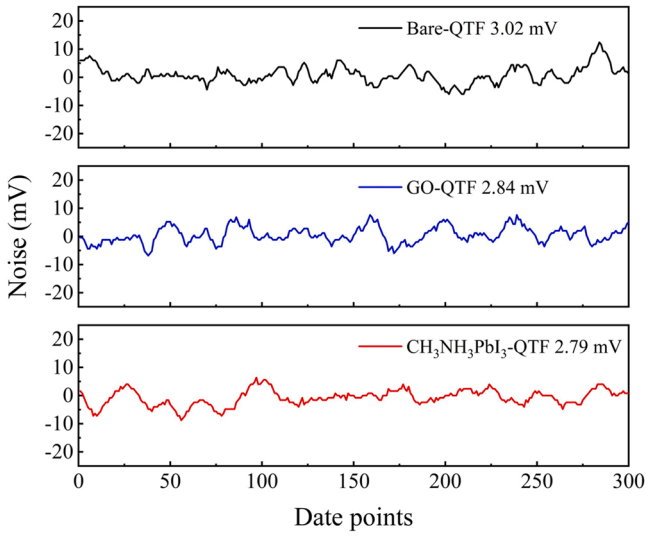

Fig. 8. The system noise of three different types of QTFs.

quality factors of 8856, 8396 and 7604, respectively. The resonance frequency and Q value of QTF coated with GO and $CH_3NH_3PbI_3$ have decreased slightly due to the fact that the resonance frequency of the QTF is very sensitive to the load mass on the QTF surface. Applying GO and $CH_3NH_3PbI_3$ to the tuning fork surface will lead to an increase in the mass quality of the QTF prong, thereby reducing the resonance frequency and the Q value.

Under the same experimental conditions, these three different kinds of QTFs were used in sequence for the experiment. First, experiments were conducted using a Bare-QTF, and the experimental results are shown in Fig. 7 (black curve) with a 2*f* signal peak of only 21.2 mV. Then, the surface of the QTF was coated with thin GO film, to enhance the absorption of laser light, and hence, to improve the thermoelastic effect of the QTF and the overall sensitivity. The experimental results are shown in Fig. 7 (blue curve), and its 2*f* signal peak is 102 mV, which is 4.81 times higher than the 2*f* signal of the Bare-QTF. Although graphene oxide improves the sensitivity by increasing the thermoelastic effect to some extent, this improvement is not enough and GO-QTF is not the best choice. Finally, we coated $CH_3NH_3PbI_3$ between two different electrodes on the surface of the QTF to form an Ag/$CH_3NH_3PbI_3$/Ag Schottky structure. The experimental results are shown in Fig. 7 (red curve), and the amplitude is as high as 2.24 V, which is ~22 times higher than that of GO-QTF and ~106 times higher than that of Bare-QTF. This is due to the $CH_3NH_3PbI_3$ perovskite has high absorption coefficient, good photoelectric effect and thermoelastic effect. The developed $CH_3NH_3PbI_3$ perovskite Schottky junction on QTF allowed the co-coupling of photoelectric effect and thermoelastic effect [41], thus greatly improving the sensitivity of LITES. In the experiment, the optimal $CH_3NH_3PbI_3$-QTF was obtained by spin-coating at 1000 rpm for 10 s, annealing and then repeated the whole process 3 more times. The coating thickness was about 400 nm, the coating presented the macrostructure of layer stacking increased the surface area when compared with that before coating, which was conducive to improve light absorption and reduce light scattering.

Fig. 8 shows the measured noise of three different kinds QTFs. The root mean square (RMS) value of Bare-QTF, GO-QTF and $CH_3NH_3PbI_3$-QTF are 3.02 mV, 2.84 mV and 2.79 mV, respectively. It can be seen that the coating film on the surface of the QTF has almost no impact on the noise level. Combining the 2*f* signal amplitude and noise, it can be calculated that the SNR of Bare-QTF, GO-QTF and $CH_3NH_3PbI_3$-QTF are 7.02, 35.92 and 802.87, respectively. The SNR of $CH_3NH_3PbI_3$-QTF is ~22 times higher than that of GO-QTF and ~114 times higher than that of Bare-QTF. The minimum detection limits (MDLs) of Bare-QTF, GO-QTF and $CH_3NH_3PbI_3$-QTF resulted 2.98%, 0.58% and 260 ppm,

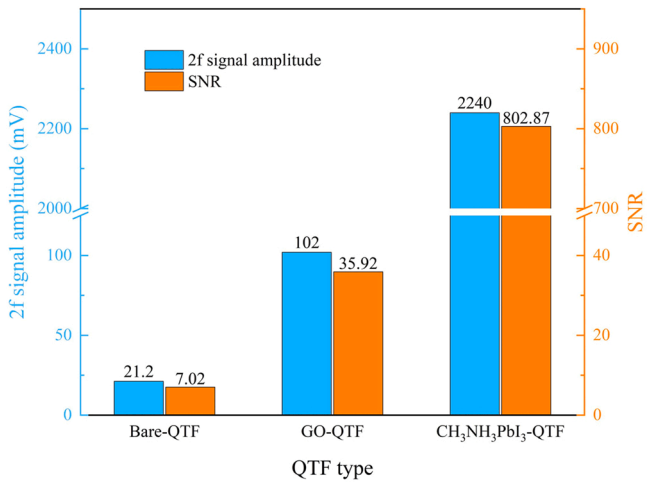

Fig. 9. 2*f* signal amplitude and SNR obtained from three different types of QTFs.

respectively. The normalized noise equivalent absorption coefficient (NNEA) of $CH_3NH_3PbI_3$-QTF is 9.21×10^{-13} $cm^{-1} \cdot W \cdot Hz^{-1/2}$. In terms of O_2 detection, Neethu et al. developed an O_2 detection TDLAS system using a 56 cm long gas cell and achieved a MDL of 0.65% [10]. Jatana et al. used a TDLAS system combined with a 4.3 m gas cell to measure O_2 concentration in a high-temperature gas stream and achieved a detection limit of 0.1% [42]. Zhou et al. used a diffused integrating cavity to increase the effective path length, and the detection limit of O_2 was up to 350 ppm [11]. Compared with the conventional TDLAS system in the literature, the detection performance of the $CH_3NH_3PbI_3$-QTF based LITES system with co-coupled thermoelastic and photoelectric effects has been significantly improved.

For the convenience of comparison, the 2*f* signal amplitude and SNR obtained by three different kinds QTFs are shown in the bar graph of Fig. 9. It can be clearly seen that the 2*f* signal amplitude and SNR of GO-QTF and $CH_3NH_3PbI_3$-QTF have been significantly improved compared to Bare-QTF, and the improvement in $CH_3NH_3PbI_3$-QTF is the most obvious, reaching two orders of magnitude. Therefore, the $CH_3NH_3PbI_3$-QTF greatly improved the detection sensitivity of the LITES system.

The response of a LITES system based on $CH_3NH_3PbI_3$-QTF under different O_2 concentrations was studied. Respectively flush O_2 of different concentrations into the gas cell and record the 2*f* signals, as shown in Fig. 10(a). The 2*f* signals as a function of O_2 concentrations are displayed in Fig. 10(b). It can be seen that the fitting curve of the 2*f* signal intensity increases with the increase of O_2 concentration. By performing a linear function fitting on the data, the R-square is 0.995. The fitting results show that the system exhibits an excellent linear response to O_2 concentration within the concentration range studied.

Allan deviation analysis is one of the simplest and most effective methods for evaluating system stability. In order to evaluate the long-term stability and detection limit of the developed LITES sensor system, 20.9% O_2 was flushed into the gas cell, and a LabVIEW controlled oscilloscope was used to continuously measure the 2*f* signal. The data sampling period was 2 s, and the total collection time was about 4 h. According to the previously obtained linear fitting curve, the Allan deviation result was converted into the oxygen concentration value. As shown in Fig. 11, the Allan deviation decreases as the average time increases. When the average time is 564 s, the MDL of the system can reach 83 ppm. In addition, the Allan bias results indicate that the main noise in the LITES sensing system comes from white noise.

It is worth noting that a smaller laser spot diameter and the optimal focusing position of the laser on the QTF surface are necessary conditions for achieving high sensitivity detection. The thermoelastic and photoelectric effects of perovskite materials are related to the power of

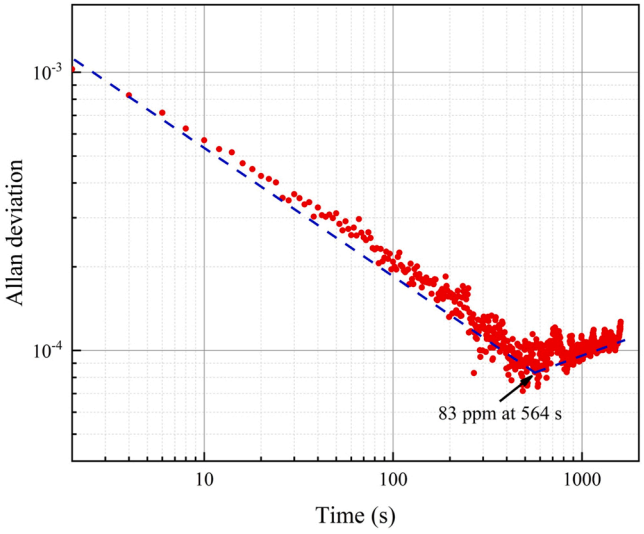

Fig. 11. Allan deviation analysis of the $CH_3NH_3PbI_3$-QTF based LITES sensor system.

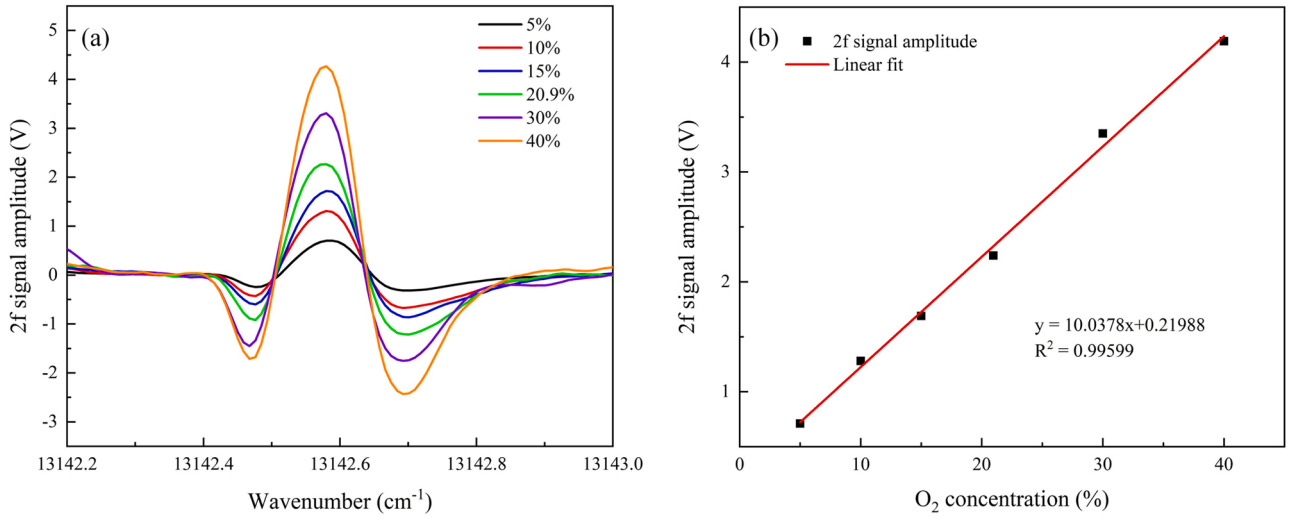

Fig. 10. (a) Experimentally measured 2*f* signals for six different concentrations of O_2. (b) The linear relationship between O_2 concentration and 2*f* signal amplitude.

the laser source. The laser used in this article has a small output power (<1 mW), and using a high-power laser may improve the MDL of the system to some extent. In addition, the absorption spectra of gases are mostly located in the infrared region, applying perovskite-QTF to other types of gas sensing may requires adjusting the absorption of perovskite to near-infrared or even mid-infrared bands. Combining perovskite with graphene to form composite materials, and combining nano gold or silver particles with perovskite to form plasma resonance may achieve this goal.

4. Conclusions

In summary, we have designed a novel $CH_3NH_3PbI_3$ perovskite-coated LITES sensor using standard commercially available QTF. By coating $CH_3NH_3PbI_3$ thin film on the surface of QTF, a Schottky junction was formed with different silver electrodes of QTF. The co-coupling of its photoelectric effect and thermoelastic effect leads to a significant improvement in detection performance. Compared with the commercial standard QTF, the introduction of $CH_3NH_3PbI_3$ perovskite material increased the 2*f* signal amplitude and SNR by ~106 and ~114 times, respectively. The MDL achieved for the $CH_3NH_3PbI_3$-QTF was 260 ppm, and the NNEA was 9.21×10^{-13} $cm^{-1}\cdot W\cdot Hz^{-1/2}$. The minimum value of Allan deviation reached to 83 ppm. This is the first time that QTF resonance detection has been combined with perovskite Schottky junctions for ultrasensitive gas detection. This method has the advantages of low cost, simple operation, and wide wavelength response range, making it a promising sensitive gas detection method.

Declaration of Competing Interest

The authors declare that they have no known competing financial interests or personal relationships that could have appeared to influence the work reported in this paper.

Data Availability

Data will be made available on request. The data that support the findings of this study are available on request from the corresponding author upon reasonable request.

Acknowledgment

This work was supported by the Hebei Province Science and Technology Support Program (Grant No. 22321701D); Department of Education of Hebei Province (Grant No. ZD2022072); Natural Science Foundation of Hebei Province (Grant No. F2021201005); National Natural Science Foundation of China (Grant No. 62275065, 62022032).

References

[1] C.S. Chu, T.W. Sung, Y.L. Lo, Portable optical oxygen sensor based on Ru(II) complex and dye entrapped core-shell nanoparticles embedded in sol-gel matrix coated on a photodiode, Opt. Eng. 50 (5) (2011), 054404, https://doi.org/10.1117/1.3581112.

[2] J. Werner, M. Belz, K.-F. Klein, T. Sun, K.T.V. Grattan, Fiber optic sensor designs and luminescence-based methods for the detection of oxygen and pH measurement, Measurement 178 (2021), 109323, https://doi.org/10.1016/j.measurement.2021.109323.

[3] Y.G. Wei, Y.S. Jiao, D. An, D.L. Li, W.S. Li, Q. Wei, Review of dissolved oxygen detection technology: from laboratory analysis to online intelligent detection, Sensors 19 (2019) 3995, https://doi.org/10.3390/s19183995.

[4] M. Li, W. Liu, J.P. Correia, A.C. Mourato, A.S. Viana, G. Jin, Optical and electrochemical combination sensor with poly-aniline film modified gold surface and its application for dissolved oxygen detection, Electroanalysis 26 (2) (2014) 374–381, https://doi.org/10.1002/elan.201300459.

[5] W.Y. Yin, J.Y. Liu, Q. Liu, J.H. Zhu, M.L. Zhang, P.L. Liu, R.M. Li, J. Wang, Double-layer carbon encapsulated co particles combined with ionic liquid for enhancing electrochemical detection of oxygen, ACS Sustain. Chem. Eng. 11 (7) (2023) 3023–3035, https://doi.org/10.1021/acssuschemeng.2c06701.

[6] H. Teichert, T. Fernholz, V. Ebert, Simultaneous in situ measurement of CO, H_2O, and gas temperatures in a full-sized coal-fired power plant by near-infrared diode lasers, Appl. Opt. 42 (12) (2003) 2043–2051, https://doi.org/10.1364/AO.42.002043.

[7] J. Chen, A. Hangauer, R. Strzoda, M.-C. Amann, Laser spectroscopic oxygen sensor using diffuse reflector based optical cell and advanced signal processing, Appl. Phys. B 100 (2010) 417–425, https://doi.org/10.1007/s00340-010-3956-3.

[8] L. Wang, Y.G. Zhang, X. Zhou, Z.G. Zhang, Sensitive dual sensing system for oxygen and pressure based on deep ultraviolet absorption spectroscopy, Sens. Actuators, B 281 (2019) 514–519, https://doi.org/10.1016/j.snb.2018.10.154.

[9] C. Zhang, S.D. Qiao, Y.F. Ma, Highly sensitive photoacoustic acetylene detection based on differential photoacoustic cell with retro-reflection-cavity, Photoacoustics 30 (2023), 100467, https://doi.org/10.1016/j.pacs.2023.100467.

[10] S. Neethu, R. Verma, S.S. Kamble, J.K. Radhakrishnan, P.P. Krishnapur, V. C. Padaki, Validation of wavelength modulation spectroscopy techniques for oxygen concentration measurement, Sens. Actuators, B 192 (2014) 70–76, https://doi.org/10.1016/j.snb.2013.10.070.

[11] X. Zhou, J. Yu, L. Wang, Q. Gao, Z.G. Zhang, Sensitive detection of oxygen using a diffused integrating cavity as a gas absorption cell, Sens. Actuators, B 241 (2017) 1076–1081, https://doi.org/10.1016/j.snb.2016.10.033.

[12] A. Pohlkötter, M. Köhring, U. Willer, W. Schade, Detection of molecular oxygen at low concentrations using quartz enhanced photoacoustic spectroscopy, Sensors 10 (9) (2010) 8466–8477, https://doi.org/10.3390/s100908466.

[13] S.D. Qiao, P.Z. Ma, V. Tsepelin, G.W. Han, J.X. Liang, W. Ren, H.D. Zheng, Y.F. Ma, Super tiny quartz-tuning-fork-based light-induced thermoelastic spectroscopy sensing, Opt. Lett. 48 (2023) 419–422, https://doi.org/10.1364/OL.482351.

[14] K. Chen, N. Wang, M. Guo, X.Y. Zhao, H.C. Qi, C.X. Li, G.Y. Zhang, L. Xu, Detection of SF_6 gas decomposition component H_2S based on fiber-optic photoacoustic sensing, Sens. Actuators, B 378 (2023), 133174, https://doi.org/10.1016/j.snb.2022.133174.

[15] K. Liu, L. Wang, T. Tan, G.S. Wang, W.J. Zhang, W.D. Chen, X.M. Gao, Highly sensitive detection of methane by near-infrared laserabsorption spectroscopy using a compact dense-pattern multipass cell, Sens. Actuators, B 370 (2022), 132429, https://doi.org/10.1016/j.snb.2022.132429.

[16] Y.H. Liu, Y.F. Ma, Advances in multipass cell for absorption spectroscopy-based trace gas sensing technology, Chin. Opt. Lett. 21 (2023), 033001, https://doi.org/10.3788/COL202321.033001.

[17] Q. Wu, H.H. Lv, L.Q. Lin, H.P. Wu, M. Giglio, W.G. Zhu, Y.C. Zhong, A. Sampaolo, P. Patimisco, L. Dong, V. Spagnolo, J.H. Yu, H.D. Zheng, Clamp-type quartz tuning fork enhanced photoacoustic spectroscopy, Opt. Lett. 47 (17) (2022) 4556–4559, https://doi.org/10.1364/OL.464334.

[18] H.Y. Lin, H.D. Zheng, B.A.Z. Montano, H.P. Wu, M. Giglio, A. Sampaolo, P. Patimisco, W.G. Zhu, Y.C. Zhong, L. Dong, R.F. Kan, J.H. Yu, V. Spagnolo, Ppb-level gas detection using on-beam quartz-enhanced photoacoustic spectroscopy based on a 28 kHz tuning fork, Photoacoustics 25 (2022), 100321, https://doi.org/10.1016/j.pacs.2021.100321.

[19] A.A. Kosterev, Y.A. Bakhirkin, R.F. Curl, F.K. Tittel, Quartz-enhanced photoacoustic spectroscopy, Opt. Lett. 27 (21) (2002) 1902–1904, https://doi.org/10.1364/OL.27.001902.

[20] Y.F. Ma, Y. He, Y. Tong, X. Yu, F.K. Tittel, Quartz-tuning-fork enhanced photothermal spectroscopy for ultra-high sensitive trace gas detection, Opt. Express 26 (24) (2018) 32103–32110, https://doi.org/10.1364/OE.26.032103.

[21] S.D. Qiao, A. Sampaolo, P. Patimisco, V. Spagnolo, Y.F. Ma, Ultra-highly sensitive HCl-LITES sensor based on a low-frequency quartz tuning fork and a fiber-coupled multi-pass cell, Photoacoustics 27 (2022), 100381, https://doi.org/10.1016/j.pacs.2022.100381.

[22] X.N. Liu, S.D. Qiao, G.W. Han, J.X. Liang, Y.F. Ma, Highly sensitive HF detection based on absorption enhanced light-induced thermoelastic spectroscopy with a quartz tuning fork of receive and shallow neural network fitting, Photoacoustics 28 (2022), 100422, https://doi.org/10.1016/j.pacs.2022.100422.

[23] X.N. Liu, Y.F. Ma, Sensitive carbon monoxide detection based on light-induced thermoelastic spectroscopy with a fiber-coupled multipass cell, Chin. Opt. Lett. 20 (3) (2022), 031201, https://doi.org/10.3788/COL202220.031201.

[24] Y.F. Ma, T.T. Liang, S.D. Qiao, X.N. Liu, Z.T. Lang, Highly sensitive and fast hydrogen detection based on light-induced thermoelastic spectroscopy, Ultrafast. Sci. 3 (2023) 0024, https://doi.org/10.34133/ultrafastscience.0024.

[25] L.E. Hu, C.T. Zheng, M.H. Zhang, K.Y. Zheng, J. Zheng, Z.W. Song, X.Y. Li, Y. Zhang, Y.D. Wang, F.K. Tittel, Long-distance in-situ methane detection using near-infrared light-induced thermo-elastic spectroscopy, Photoacoustics 21 (2021), 100230, https://doi.org/10.1016/j.pacs.2020.100230.

[26] L.E. Hu, C.T. Zheng, Y. Zhang, J. Zheng, Y.D. Wang, F.K. Tittel, Compact all-fiber light-induced thermoelastic spectroscopy for gas sensing, Opt. Lett. 45 (7) (2020) 1894–1897, https://doi.org/10.1364/OL.388754.

[27] K.Y. Zheng, C.T. Zheng, L.E. Hu, G.Y. Guan, Y.M. Ma, F. Song, Y. Zhang, Y. D. Wang, F.K. Tittel, Light-induced off-axis cavity-enhanced thermoelastic spectroscopy in the near-infrared for trace gas sensing, Opt. Express 29 (15) (2021) 23213–23224, https://doi.org/10.1364/OE.430745.

[28] Q.D. Zhang, W.H. Gong, J. Chang, Y.B. Wei, T.T. Zhang, Z.W. Wang, Y.F. Li, W. H. Zhang, T.Y. Liu, Long-distance free space gas detection system based on QEPTS technique for CH_4 leakage monitoring, Infrared Phys. Technol. 122 (2022), 104091, https://doi.org/10.1016/j.infrared.2022.104091.

[29] S.D. Russo, A. Zifarelli, P. Patimisco, A. Sampaolo, T.T. Wei, H.P. Wu, L. Dong, V. Spagnolo, Light-induced thermo-elastic effect in quartz tuning forks exploited as a photodetector in gas absorption spectroscopy, Opt. Express 28 (13) (2020) 19074–19084, https://doi.org/10.1364/OE.393292.

[30] T.T. Wei, H.P. Wu, L. Dong, R.Y. Cui, S.T. Jia, Palm-sized methane TDLAS sensor based on a mini-multi-pass cell and a quartz tuning fork as a thermal detector, Opt. Express 29 (8) (2021) 12357–12364, https://doi.org/10.1364/OE.423217.

[31] Y.F. Ma, Y. He, P. Patimisco, A. Sampaolo, S.D. Qiao, X. Yu, F.K. Tittel, V. Spagnolo, Ultra-high sensitive trace gas detection based on light-induced thermoelastic spectroscopy and a custom quartz tuning fork, Appl. Phys. Lett. 116 (2020), 011103, https://doi.org/10.1063/1.5129014.
[32] M. Duquesnoy, G. Aoust, J.-M. Melkonian, R. Lévy, M. Raybau, A. Godard, Quartz enhanced photoacoustic spectroscopy based on a custom quartz tuning fork, Sensors 19 (6) (2019) 1362, https://doi.org/10.3390/s19061362.
[33] S.D. Qiao, Y.F. Ma, Y. He, P. Patimisco, A. Sampaolo, V. Spagnolo, Ppt level carbon monoxide detection based on light-induced thermoelastic spectroscopy exploring custom quartz tuning forks and a mid-infrared QCL, Opt. Express 29 (16) (2021) 25100–25108, https://doi.org/10.1364/OE.434128.
[34] S. Zhou, K. Chen, L.G. Xu, B.L. Yu, T.T. Jiang, J.S. Li, Ultrathin two-dimensional Fe-doped cobaltous oxide as a piezoelectric enhancement mechanism in quartz crystal tuning fork (QCTF) photodetectors, Opt. Lett. 46 (3) (2021) 496–499, https://doi.org/10.1364/OL.406103.
[35] C.G. Lou, X. Yang, X.T. Li, H.J. Chen, C. Chang, X.L. Liu, Graphene-enhanced quartz tuning fork for laser-induced thermoelastic spectroscopy, IEEE Sens. J. 21 (8) (2021) 9819–9824, https://doi.org/10.1109/JSEN.2021.3059905.
[36] C.G. Lou, X.T. Li, H.J. Chen, X. Yang, Y. Zhang, J.Q. Yao, X.L. Liu, Polymer-coated quartz tuning fork for enhancing sensitivity of laser-induced thermoelastic spectroscopy, Opt. Express 29 (8) (2021) 12195–12205, https://doi.org/10.1364/OE.421356.
[37] C.G. Lou, H.J. Chen, X.T. Li, X. Yang, Y. Zhang, J.Q. Yao, Y.F. Ma, C. Chao, X.L. Liu, Graphene oxide and polydimethylsiloxane coated tuning fork for improved sensitive near-and mid-infrared detection, Opt. Express 29 (13) (2021) 20190–20204, https://doi.org/10.1364/OE.428003.
[38] I.E. Gordon, L.S. Rothman, C. Hill, R.V. Kochanov, Y. Tan, P.F. Bernath, M. Birk, V. Boudon, A. Campargue, K.V. Chance, B.J. Drouin, J.M. Flaud, R.R. Gamache, J. T. Hodges, D. Jacquemart, V.I. Perevalov, A. Perrin, K.P. Shine, M.A.H. Smith, J. Tennyson, G.C. Toon, H. Tran, V.G. Tyuterev, A. Barbe, A.G. Császár, V.M. Devi, T. Furtenbacher, J.J. Harrison, J.M. Hartmann, A. Jolly, T.J. Johnson, T. Karman, I. Kleiner, A.A. Kyuberis, J. Loos, O.M. Lyulin, S.T. Massie, S.N. Mikhailenko, N. Moazzen-Ahmadi, H.S.P. Müller, O.V. Naumenko, A.V. Nikitin, O.L. Polyansky, M. Rey, M. Rotger, S.W. Sharpe, K. Sung, E. Starikova, S.A. Tashkun, J. Vander-Auwera, G. Wagner, J. Wilzewski, P. Wcisło, S. Yu, E.J. Zak, The HITRAN 2016 molecular spectroscopic database, J. Quant. Spectrosc. Radiat. Transf. 203 (2017) 3–69, https://doi.org/10.1016/j.jqsrt.2017.06.038.
[39] V.H. Payne, B.J. Drouin, F. Oyafuso, L. Kuai, B.M. Fisher, K. Sung, D. Nemchick, T. J. Crawford, M. Smyth, D. Crisp, E. Adkins, J.T. Hodges, D.A. Long, E.J. Mlawer, A. Merrelli, E. Lunny, C.W. O'Dell, Absorption coefficient (ABSCO) tables for the Orbiting Carbon Observatories: Version 5.1, J. Quant. Spectrosc. Radiat. Transf. 255 (2020), 107217, https://doi.org/10.1016/j.jqsrt.2020.107217.
[40] Y. He, Y.F. Ma, Y. Tong, X. Yu, F.K. Tittel, Ultra-high sensitive light-induced thermoelastic spectroscopy sensor with a high Q-factor quartz tuning fork and a multipass cell, Opt. Lett. 44 (8) (2019) 1904–1907, https://doi.org/10.1364/OL.44.001904.
[41] C.G. Lou, J.L. Dai, Y.X. Wang, Y. Zhang, Y.F. Li, X.L. Liu, R.K. Li, Y.F. Ma, Quartz tuning fork-based high sensitive photodetector by co-coupling photoelectric and the thermoelastic effect of perovskite, Opt. Express 31 (6) (2023) 10027–10037, https://doi.org/10.1364/OE.485411.
[42] G.S. Jatana, A.K. Perfetto, S.C. Geckler, W.P. Partridge, Absorption spectroscopy based high-speed oxygen concentration measurements at elevated gas temperatures, Sens. Actuators, B 293 (2019) 173–182, https://doi.org/10.1016/j.snb.2019.04.143.

Cunguang Lou received the Ph.D. degree from South China Normal University, Guangzhou, China, in 2012. From 2012–2015, he was an Assistant Professor with the College of Biophotonics, South China Normal University. He is currently an Associate Professor with the College of Electronic Information Engineering, Hebei University. From 2017–2022, he has been a Postdoctoral Researcher with the College of Precision Instruments and Optoelectronic Engineering, Tianjin University. His research interests are the optical gas sensor and terahertz spectroscopy.

Jialiang Dai received the B.S. degree in automation from Cangzhou Normal University, Hebei, China, in 2021. He is currently pursuing the M.S. degree with the Institution of Electronic and Information Engineering, Hebei University, Hebei. His current research interests include optical gas sensing, light-induced thermoelastic spectroscopy, and quartz enhanced photoacoustic spectroscopy.

Yaxin Wang received the B.S. degree in automation from the Industrial and Commercial College, Hebei University, Hebei, China, in 2020, where he is currently pursuing the M.S. degree with the Institution of Electronics and Information Engineering. His current research interests include optical gas sensing and quartz enhanced photoacoustic spectroscopy

Yu Zhang received the Ph.D. degree from the Department of Optical Engineering, Hebei University, Hebei, China, in 2020, where she is currently an Assistant Professor with the Department of Electronics and Information Engineering. Her research interests include two-dimensional materials, solar cells, and photovoltaic technologies.

Yifan Li received the Ph.D. degree from the College of Precision Instruments and Optoelectronic Engineering, Tianjin University, Tianjin, China, in 2021. She is currently an Assistant Professor with the Department of Electronics and Information Engineering. Her research interests include two-dimensional materials and photovoltaic technologies.

Xiuling Liu received the B.S. and M.S. degrees from Tianjin University, Tianjin, China, in 1999 and 2002, and received the Ph.D. degree from the Department of Optical Engineering, Hebei University, Hebei, China, in 2010. She is currently a Professor with the Department of Electronic and Information Engineering. Her research interests include virtual reality, biomedical imaging, and signal processing.

Yufei Ma received his Ph.D. degree in physical electronics from Harbin Institute of Technology, China, in 2013. From September 2010 to September 2011, he spent as a visiting scholar at Rice University, USA. Currently, he is a professor at Harbin Institute of Technology, China. He is the winner of National Outstanding Youth Science Fund. His research interests include optical sensors, trace gas detection, laser spectroscopy, solid-state laser and optoelectronics. He has published more than 100 publications and given more than 20 invited presentations at international conferences. He serves as associate editor for Optica Optics Express, SPIE Optical Engineering, Wiley Microwave and Optical Technology Letters and Frontiers in Physics. He also serves as topical editor for CLP Chinese Optics Letters and editorial board member for Elsevier Photoacoustics MDPI Sensors and Applied Sciences.